Journal of Peptide Science
J. Peptide Sci. **8**: 365–372 (2002)
Published online in Wiley InterScience (www.interscience.wiley.com). DOI: 10.1002/psc.399

Study of the Yeast *Saccharomyces cerevisiae* F_1F_O-ATPase ε-Subunit

CÉLINE AZNAR-DERUNES,[a] CLAUDE MANIGAND,[a] PHILIPPE PICARD,[a]* ALAIN DAUTANT,[a] MICHAEL GOETZ,[b] JEAN-MARIE SCHMITTER[b] and GILLES PRECIGOUX[a]

[a] Unité de Biophysique Structurale, UMR 5471 CNRS, Université Bordeaux 1, Talence, France
[b] Institut Européen de Chimie et Biologie, FRE 2247 CNRS, ENSCPB, Talence, France

Received 11 February 2002
Accepted 25 March 2002

Abstract: The yeast *Saccharomyces cerevisiae* F_1F_O-ATPase ε-subunit (61 residues) was synthesized by the solid-phase peptide approach under both acidic and basic strategies. Only the latter strategy allowed us to obtain a pure ε-subunit. The strong propensity of the protein to produce few soluble dimeric species depending on pH has been proved by size-exclusion chromatography, electrophoresis and mass spectrometry. A circular dichroism study showed that an aqueous solution containing 30% trifluoroethanol or 200 mM sodium dodecyl sulphate is required for helical folding. In both solvents at acidic pH, the ε-subunit is soluble and monomeric.

Keywords: circular dichroism; ε-subunit; mitochondrial F_1F_O-ATPase; peptide synthesis

INTRODUCTION

Of the molecules able to retain and to provide living cells with usable energy the most important is ATP. The F_1F_O-ATPase enzyme ensures its synthesis from ADP and Pi [1,2]. F_1F_O-ATPase is located in the inner mitochondrial or chloroplast membrane of eukaryotic cells and in the plasma membrane of bacteria. Its modern description is based on numerous biochemical and biophysical studies [3–8]. It is composed of two sectors: one is hydrophilic, F_1, where ATP formation or hydrolysis takes place; the other, F_O, is hydrophobic and embedded in the membrane. A central stalk (commonly constituted by γ- and δ-subunits in a 1 : 1 ratio) and an external arm connect the catalytic head of F_1 (always constituted by α- and β-subunits in the ratio 3 : 3) to the membranous base of F_O (constituted at least by a ring of 9–12 *c*-subunits and by one *a*-subunit). Depending on the organism, several subunits are added to these two sectors.

The elucidation of ATP synthase function is in progress. Electron flow in the respiratory chain originates from a proton translocation that creates a pH gradient across the inner mitochondrial or plasma membrane. This proton flow passes through the membranous sector of ATP synthase and drives the rotation of the *c*-subunit ring, which involves the central stalk rotation. However, the $(\alpha\beta)_3$ catalytic head, which interacts strongly with this stalk (essentially through the γ-subunit), cannot undergo a rotation since the external arm freezes it. Then, the catalytic sites, located at the α- and β-subunit interfaces, undergo a conformational modification that induces their affinity for the different substrates to change [6,8–11].

Abbreviations: DCC, 1,3-dicyclohexylcarbodiimide; DIEA, diisopropylethylamine; DMF, *N*,*N*-dimethylformamide; DMSO, dimethylsulphoxide; ESI, electrospray ionization; Fmoc, 9-fluorenylmethyloxycarbonyl; HBTU, O-benzotriazol-1-yl-*N*,*N*,*N*′,*N*′-tetramethyluronium; HOBt, 1-hydroxy-benzotriazole; NMP, 1-methyl-2-pyrrolidinone; NMR, nuclear magnetic resonance; PAM, phenylacetamidomethyl; SDS, sodium dodecylsulphate; *t*-Boc, *tert*-butyloxycarbonyl; TFA, trifluoroacetic acid; TFE, 2,2,2-trifluoroethanol.

*Correspondence to: Dr Philippe Picard, Unité de Biophysique Structurale, Bât B8, avenue des Facultés, Université Bordeaux I, 33405 Talence Cedex, France; e-mail: P.Picard@ubs.u-bordeaux.fr

Identification of the F_1 and F_O subunits implicated in these local rearrangements is a current goal. For this reason, the central stalk is of great interest. In mitochondria this stalk contains a third supernumerary protein, the ε-subunit. It is not essential to the ATP synthase assembly but its absence in yeast, induced by the ATP15 gene disruption, promotes a proton leak and inhibits oxidative phosphorylation [12,13]. Thus, the function of the ε-subunit in energy mechanism is important and has still to be clarified.

This paper is aimed at the preparation of the ε-subunit in a pure state and in a sufficient amount to allow future structural and biochemical studies. Determination of the conditions that allow the solubilization and structuring of the synthetic protein is also reported.

MATERIALS AND METHODS

All solvents, reagents, *t*-Boc- and Fmoc- protected amino acids and resins were purchased from SDS (Peypin, France), Sigma-Aldrich (St Quentin Fallavier, France) and Novabiochem (Läufelfingen, Switzerland), respectively.

Solid-Phase Peptide Synthesis

t-Boc chemistry. Chemical synthesis was performed on an Applied Biosystems 431A synthesizer (Courtaboeuf, France), starting from the *t*-Boc-L-Lys(2-chlorobenzyloxycarbonyl)-PAM-resin. N^{α}-*t*-Boc-amino acids with reactive side-chain groups were used protected as follows: Arg (tosyl); Lys (2-chlorobenzyloxycarbonyl); Asp, Glu (cyclohexyl); Ser, Thr (benzyl); Tyr (2-bromobenzyloxycarbonyl). A 20-fold excess of each protected *t*-Boc-amino acid was employed. Activation and coupling were achieved in NMP with 1 M HOBt and 1 M DCC, respectively. A capping step was performed after each coupling with 10% acetic anhydride and 5% DIEA in NMP (v/v). Peptide/resin cleavage and simultaneous deprotection of the side-chain groups were carried out by classical pure HF treatment. The crude polypeptide was stored at 4 °C after lyophilization.

Fmoc chemistry. The automatic synthesizer used was an Applied Biosystems 433A (Courtaboeuf, France) equipped with a conductivity measurement monitor system. The protecting groups of the side chains were: Arg (2,2,5,7,8-pentamethylchroman-6-sulfonyl); Lys (*t*-Boc); Asn, Gln (trityl); Asp, Glu (O-*t*-butyl); Ser, Thr, Tyr (*t*-butyl). N^{α}-protected Fmoc-amino acids were introduced in a 5-fold excess compared with the Fmoc-L-Lys(*t*-Boc)-Novasyn®-TGA resin (0.19 mmol/g). Coupling was performed with a solution of HBTU/HOBt (0.50/0.45 M) in DMF and the coupling time was increased compared with the classical protocol to reach 40 min. A capping step was performed with a solution of 4.75% acetic anhydride, 2.25% DIEA (v/v) and 15 mM HOBt in NMP. Peptide/resin cleavage and side-chain group deprotection were performed simultaneously with a solution made of 10 ml TFA, 0.75 g phenol, 0.25 ml 1,2-ethanedithiol, 0.5 ml thioanisole and 0.5 ml deionized water. Then, the peptide solution was lyophilized and the crude peptide stored at 4 °C.

RP-HPLC Purification

The crude peptide was solubilized in 0.1% TFA in water and RP-HPLC was performed on a Waters 600E system (St Quentin en Yveline, France) equipped with a Waters 996 photodiode array detector (220 nm) (St Quentin en Yveline, France). A C_{18} Vydac semi-preparative column (10 × 250 mm, 300 Å, 5 μm) was employed. Two successive purification steps were necessary using the two eluants A (0.1% TFA in water) and B (0.08% TFA in acetonitrile); the first step was with a linear gradient from 20% to 80% B for 30 min at 3 ml/min flow rate, and the second step was under the following conditions: an isocratic 70%/30% A/B mixture during 10 min followed by a linear gradient bringing the eluant B proportion to 50% during 30 min at 3 ml/min flow rate. Control of the purification steps was performed on a C_{18} Vydac analytical column (4.6 × 250 mm, 300 Å, 5 μm) at 1 ml/min flow rate using the purification gradients.

Size-Exclusion Chromatography (SEC)

A Superdex 200 HR 10/30 column (10 × 300 mm) (Amersham Pharmacia Biotech, Orsay, France) and a Waters Alliance apparatus coupled with a mono-λ Waters 486 detector (220 nm) were employed. Elution was achieved at 0.7 ml/min flow rate. Different 50 mM buffers containing 150 mM NaCl used as eluant were: glycine (pH 10.4), Tris-HCl (pH 8.4) and phosphate (pH 6.8). Two other eluants at pH 4.7 and 3.4 were obtained by acidification of the phosphate buffer. Samples were prepared by dissolution of peptide aliquots in the different saline

solutions followed by centrifugation to eliminate the unsolubilized peptide species. For every peptide sample analysed the injection volume was 10 µl. Elution profiles were scaled by means of a molecular mass standard (Bio-Rad Gel Filtration Standard, Yvry sur Seine, France).

SDS-PAGE

Tricine gel electrophoreses were performed on a Mini-Protean II (Bio-Rad) during 3 h at a 100 V constant voltage. 15 µl of peptide solution mixed with 15 µl of denaturant buffer containing 2% SDS were loaded. Calibration was performed with molecular mass standards (Sigma Myosin Kit). Peptides were visualized by staining with silver nitrate [14].

Mass Spectrometry

Mass spectra were recorded on a LCT of instrument (Micromass, Manchester, UK), equipped with an electrospray source and time-of-flight analyser, and were deconvoluted. Measurements were carried out in an external calibration mode by using the horse heart apomyoglobin multi-charged ion spectrum. Peptides dissolved (10 µM) in a water/methanol (1 : 1, v/v) mixture containing 1% (v/v) acetic acid were introduced by infusion at a 5 µl/min constant flow rate with a syringe pump (Fisher Scientific, Elancourt, France).

Far-UV and Near-UV CD Spectroscopy

CD studies were performed at room temperature on a Mark VI Jobin-Yvon dichrograph (Longjumeau, France) with a cell of 1 mm pathlength (increment 0.5 nm, bandwidth 2 nm, integration time 2 s). The Fmoc-peptide concentrations and wavelength ranges were 30 µM and 184 to 270 nm for the far-UV CD, and 300 µM and 260 to 310 nm for the near-UV CD. At these concentrations the peptide solutions were clear and did not need centrifugation. The ellipticity is reported in terms of $[\theta]_R$, residue molar value.

RESULTS

ε-Subunit Preparation and Water Solubility

t-Boc chemistry. Synthesis of the 61-residue peptide [12] (sequence displayed in Figure 1) was performed using acid strategy with a single coupling. The ESI-MS deconvoluted spectrum (Figure 2a), carried out after RP-HPLC purifications, revealed the presence of two truncated and acetylated minor peptides (approximately <8%): Ac-L^{14}-K^{61} (average mass exp.: 5228.0 ± 0.7 Da, calcd. mass: 5227.78 Da) and Ac-S^{9}-K^{61} (average mass exp.: 5786.5 ± 0.7 Da, calcd. mass: 5783.40 Da), besides the expected polypeptide (average mass exp.: 6611.5 ± 0.7 Da, calcd. mass: 6611.39 Da). Further purification by anion-exchange chromatography (Waters Protein-Pak AP-1 SP 15HR column, 10 × 100 mm) at pH 7.1 (pHi 9.77) was unsuccessful, the ε-subunit still being co-eluted (0.2 M NaCl) with these two contaminants (data not shown). Therefore, another synthesis was performed with a double coupling for the 14 *N*-terminal residues and the coupling time

```
                    1         10         20         30         40         50         60
                    |         |          |          |          |          |          |
yeast sequence  : -SAWRKAGISYAAYLNVAAQAIRSSLKTELQTASVLNRSQTDAFYTQYKNGTAASEPTPITK
nnpredict       : -----HH-HHHHHHHHHHHHHHHH--HHHHHHHHEE-------HHEE---------------
PSSP/SSP        : -HHHHHH---HHHHHHHHHHHHHHHHHHHHHHHHHHHH--HHHHHHHH-------------H
PSSP/nnSSP      : -------HHHHHHHHHHHHHHHHH-----------------HHHHHHHHH------------
PHDsec          : ---------HHHHHHHHHHHHHHHHHHHHHHHHHHHHHH--HHHHHHHHH-------------
PSA             : ---------HHHHHHHHHHHHHHHHHHHHHHHHHHHHH--HHHHHHHHH-----HHH-------
X-ray structure: -hhhhhhhh-HHHHHHHHHHHHHH---hhh-hhhhhhhh----EEEE------
bovine sequence: VAYWRQAGLSYIRYSQICAKAVRDALKTEF-KANAMKTSGSTIKIVK-VKKEK
                    |         |          |          |          |          |
                    1         10         20         30         40         50
```

Figure 1 Sequences of *S. cerevisiae* (yeast) and bovine ε-subunit (lines 1 and 8, respectively). Secondary structure predictions for *S. cerevisiae* ε-subunit (http://www.expasy.ch/tools/) (lines 2–6). X-ray diffraction structure of bovine ε-subunit (line 7). H and h, helices; E, strand; dash, no prediction; PSSP/SSP, protein secondary structure prediction/segment-oriented structure prediction; PHDsec, Profil network prediction Heidelberg determination secondary structure; PSA, protein sequence analysis.

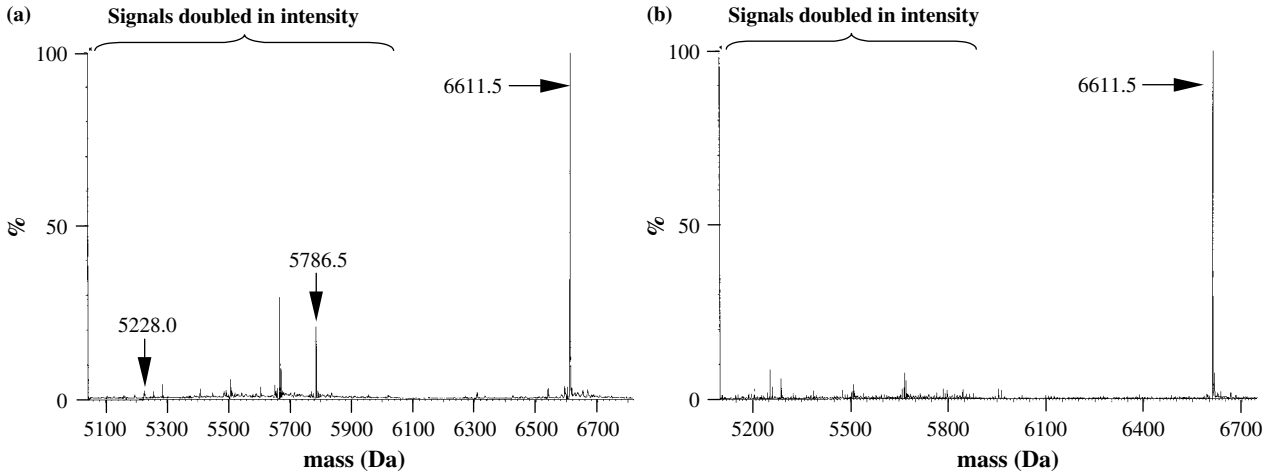

Figure 2 ESI deconvoluted mass spectra of *t*-Boc (a) and Fmoc (b) peptides after RP-HPLC purification. Peaks corresponding to peptides are indicated by an arrow; the other peaks are artefacts due to deconvolution calculations.

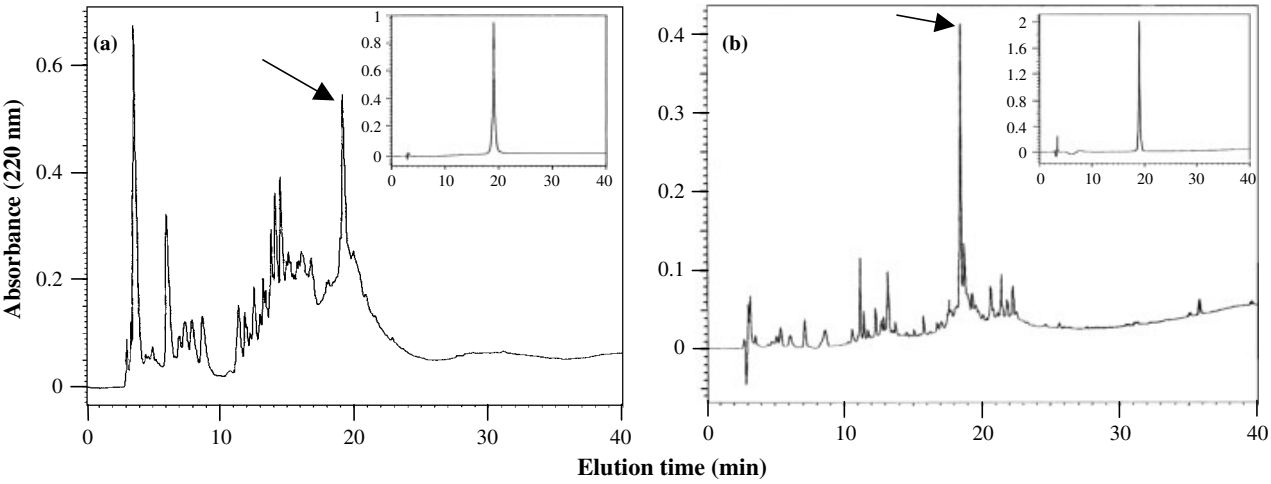

Figure 3 Analytical RP-HPLC chromatograms of the crude *t*-Boc (a) and Fmoc (b) peptides. Insets: chromatograms of peptides after *semi*-preparative RP-HPLC purifications.

increased by 20 min and 10 min after the introduction of 15% DMSO solution and 1% DIEA solution, respectively. Unfortunately, this procedure did not provide a peptide free of truncated species.

At 3 mM, a minimal concentration required to undertake structural studies by NMR on a 400 MHz apparatus, the aqueous solution of the *t*-Boc-peptide (pH 3.4) was turbid. The presence of truncated peptides could be one of the reasons for this finding.

Fmoc chemistry. The analytical RP-HPLC chromatogram of the Fmoc crude peptide showed less numerous impurities and in a reduced proportion compared with the *t*-Boc crude peptide (Figure 3). After RP-HPLC purification mass spectrometry allowed the identification of the peptide (40 mg) as the pure ε-subunit (average mass exp.: 6611.4 ± 0.7 Da, calcd. mass: 6611.39 Da) (Figure 2b). However, preparation of an aqueous solution of the pure Fmoc polypeptide at 3 mM concentration was unsuccessful.

Evidence for Dimeric Species in Aqueous Medium

This study was performed by SEC as a function of pH at a 3 mM peptide concentration.

Firstly, the *t*-Boc peptide behaviour was studied. At pH 3.4 the chromatogram profile showed a main peak and a shoulder corresponding to estimated

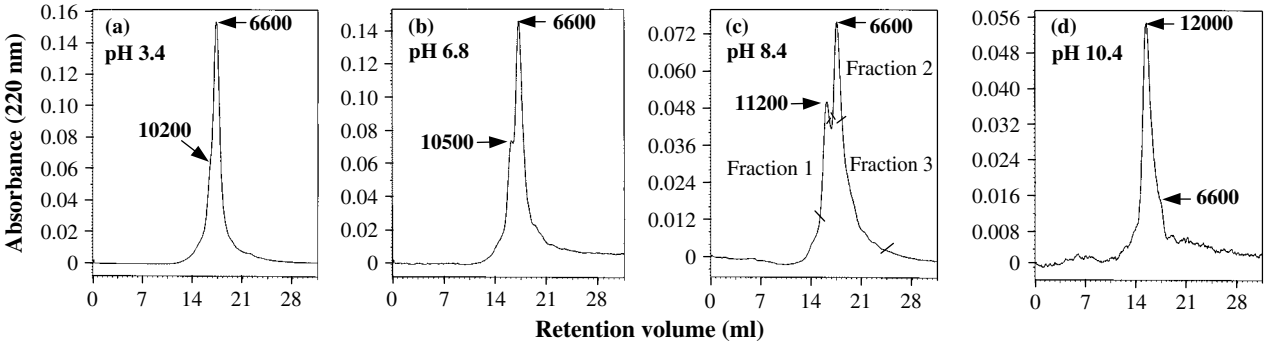

Figure 4 SEC chromatograms of *t*-Boc peptide dissolved at different pH and at 3 mM concentration. The oblique lines in (c) indicate the limits of the different fractions collected.

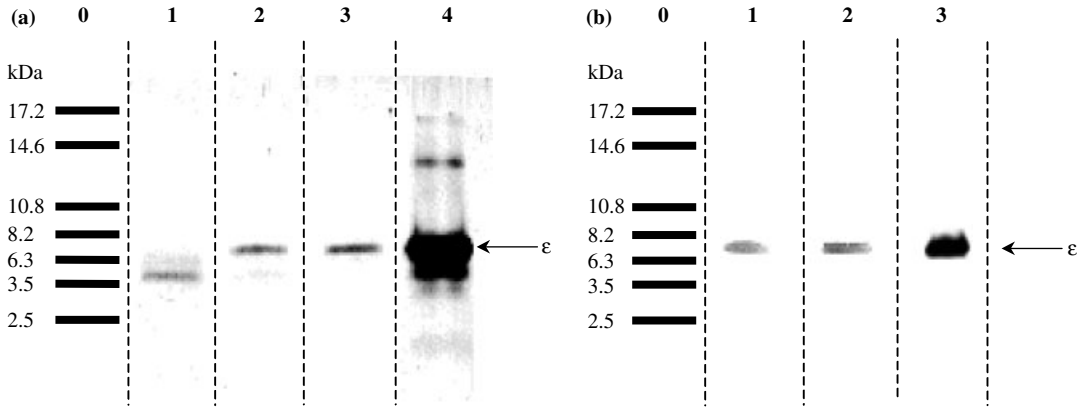

Figure 5 (a) Tricine SDS-PAGE of three SEC fractions of *t*-Boc peptide. Lane 0: molecular mass standards; lanes 1 to 3: fractions 1 to 3; lane 4: *t*-Boc peptide before SEC separation. (b) Tricine SDS-PAGE of two SEC fractions of Fmoc peptide. Lane 0: molecular mass standards; lanes 1 and 2: fractions 1 and 2; lane 3: Fmoc peptide before SEC separation.

masses of 6600 ± 600 Da and $10\,200 \pm 600$ Da, respectively (Figure 4a). When the pH was increased, the main peak intensity decreased (Figure 4a–d) becoming a small shoulder at pH 10.4 (the concentration was ten times lower than that observed at pH 3.4). In order to identify the corresponding species, three fractions were collected at pH 8.4 (Figure 4c), concentrated (using ultrafiltration membranes) and analysed under denaturing conditions by SDS-PAGE (Figure 5a) and ESI-MS (results not shown). The results, combined with the mass values determined by SEC, allowed us to conclude that fraction 1 contained mainly homo- or heterodimers of truncated peptides, while fractions 2 and 3 contained the ε-subunit in a monomeric form. Truncated peptides were not seen in fraction 3, where their presence as a monomer was expected. By ESI-MS a weak signal indicative of the ε-subunit was detected in fraction 1; nevertheless, the overlap of fractions 1 and 2 did not allow the determination of whether the ε-subunit was present in a monomeric or dimeric state. The decreasing population of the dissolved ε-subunit as a function of the pH was probably due to the formation of dimeric species that are sparingly soluble. The observation of an increase of the second peak mass (determined by SEC), when the pH was raised (Figure 4a–d), is in favour of this hypothesis.

Secondly, the Fmoc peptide behaviour was studied at pH 8.4: two fractions were collected (Figure 6), concentrated and analysed under denaturing conditions by SDS-PAGE (Figure 5b) and ESI-MS (results not shown). Figures 6 and 5b support the previously advanced hypothesis concerning the ability of the ε-subunit to form dimers in aqueous medium. However, the absence of truncated peptides led in this case to a lower amount of associated species (compare Figure 6 with Figure 4c). The influence of pH on dimerization was confirmed (results not shown).

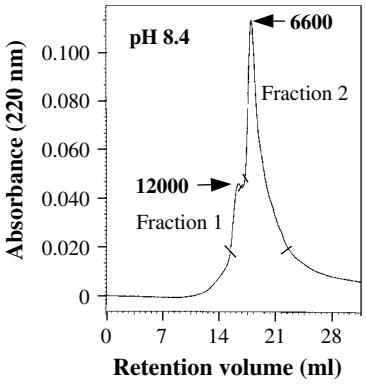

Figure 6 SEC chromatogram of Fmoc peptide at pH 8.4 and 3 mM concentration. The oblique lines indicate the limits of the different fractions collected.

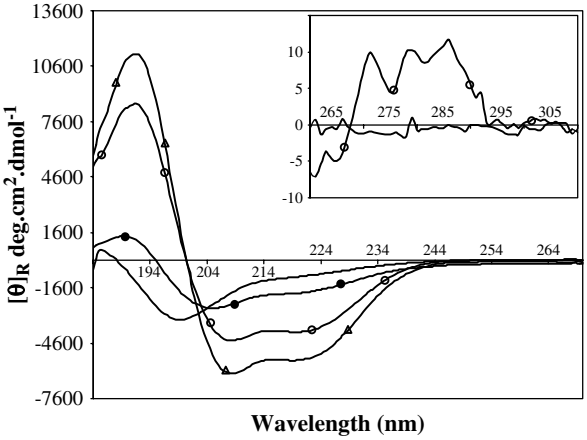

Figure 7 Far-UV CD spectra of Fmoc peptide in water (thin line) and in 90% water–10% TFE (full circles), 70% water–30% TFE (empty circles), and 50% water–50% TFE (triangles). Inset: near-UV CD spectra in water (thin line) and 70% water–30% TFE (empty circles).

Structuring and Non-associating Solvents

A far-UV CD study of an aqueous solution of 30 μM Fmoc peptide indicated that the ε-subunit is unfolded (negative band at 200 nm typical of a random-coil conformation) (Figure 7). Therefore, a solvent was looked for that would allow the ε-subunit to be folded and dissolved at a 3 mM concentration.

The Fmoc peptide, solubilized at different TFE percentages (0 to 50%) in water, showed that an helical folding gradually took place as indicated by the CD spectral evolution (Figure 7). The percentages of secondary structure elements, calculated by the singular value decomposition method [15], are reported in Table 1. As the increase of TFE concentration could be responsible for the loss of tertiary structure in favour of secondary structure [16], near-UV CD experiments were performed. They led to clear evidence for a tertiary structure (aromatic amino acids involved: probably W^3, Y^{10} and Y^{13}), up to 30% TFE (inset in Figure 7). In a 50 : 50 water/TFE solution, the 3D-assembly disappeared (result not shown).

At 3 mM concentration the Fmoc peptide solubilized in 70% water/30% TFE (pH 3.4) gave a clear solution without any associated species, as confirmed by SEC (Figure 8a). Moreover, the amount of dissolved ε-subunit remained stable over time. The SEC performed on the *t*-Boc peptide solubilized

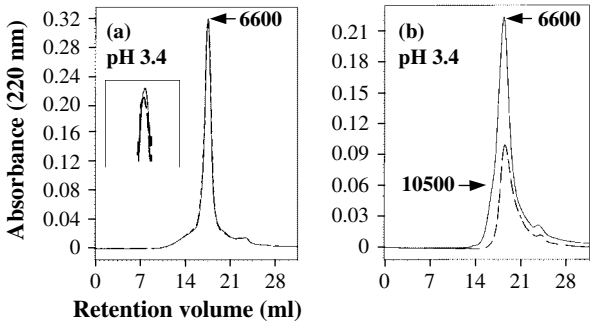

Figure 8 SEC chromatograms of Fmoc (a) and *t*-Boc (b) peptides in 70% water/30% TFE at pH 3.4 and 3 mM concentration after 5 min (solid line) and 24 h (dashed line). Inset: zoom of the peak top.

Table 1 Percentages of Secondary Structures Calculated from X-ray Structure (a) and far-UV CD Spectra (b)

	(a) Beef heart ε-subunit (1E79)	(b) Pig heart ε-subunit	(b) Synthesized *S. cerevisiae* ε-subunit in water containing:			
			10% TFE	30% TFE	50% TFE	200 mM SDS
Helices	27	24	14	38	51	22
Sheets	8	11	18	17	10	15
Turns	37	12	25	19	17	24
Others	28	53	43	26	22	39

in 70% water/30% TFE revealed the presence of a small amount of dimeric species, but unfortunately the ε-subunit concentration decreased over time (Figure 8b), indicating an increasing association.

To extend the research to other non-associating and structuring solvent mixtures, a detergent (200 mM SDS) was used. The Fmoc peptide solution obtained at 3 mM concentration (pH 4.6) was clear. SEC (result not shown) confirmed the absence of any associated species (the same results were obtained with the *t*-Boc peptide). A chromatographic peak corresponding to a 8300 ± 600 Da mass was observed, indicating that the ε-subunit is interacting with the SDS molecules. Under these conditions 2D (Table 1) and 3D (result not shown) helical folding of the ε-subunit was clearly established by CD spectroscopy.

DISCUSSION

Biochemical and structural biophysical studies require significant amounts of protein samples. Over-expression of the ε-subunit in *E. coli* (wild-type or fused with glutathione-S-transferase) was unsuccessful. Isolation from a yeast *S. cerevisiae* 20 l culture produced only a few µg of the protein [12]. As SPPS generally leads to large amounts of small proteins, this procedure has been researched. Acidic chemistry allowed the synthesis of the desired peptide, but contamination by two truncated peptides has been observed after RP-HPLC and ion-exchange purifications. Fmoc chemistry has also been performed. A resin with a low substitution rate (between 0.1 and 0.3 mmol/g) was chosen owing to the peptide length. In addition, a Novasyn®-TGA-resin was used as the polyethyleneglycol spacer prevents the hiding of α-amino terminal function due to folding. All these modifications to the synthetic conditions employed led to a pure peptide.

The absence of an ordered secondary structure observed for the ε-subunit in an aqueous solution did not agree with the secondary structure predictions as deduced from the x-ray diffraction structure of the homologous bovine mitochondrial ε-subunit (51 residues) in the F_1 sector [8] and from the CD results of the pig heart ε-subunit (50 residues) [17]. The denaturating conditions (0.1% TFA) of chemical synthesis and RP-HPLC purifications could explain such a result [18]. Dissolution in aqueous solution is not sufficient to correctly refold the protein after these purification steps. TFE is a solvent well known for its ability to stabilize nascent secondary structures (helices and β-sheets) [19,20]. In the presence of TFE the strength of intermolecular hydrophobic interactions decreases and the number of intramolecular hydrogen bond increases. The results obtained in the present study confirm this propensity. Moreover, the loss of the ε-subunit tertiary structure in the presence of 50% TFE is also in agreement with previous observations [16]. The difference of helix proportion observed by CD in 70% water/30% TFE and in 200 mM SDS (Table 1) could be explained by the strong propensity of the TFE to induce intramolecular hydrogen bonds in peptides, followed by helix formation.

To understand the high tendency of the pure ε subunit for homo-dimerization in aqueous solutions, the Kyte-Doolittle [21] hydrophobicity profile was determined (data not shown). The profile was hydrophobic from residues 9–22 and 30–34. These hydrophobic areas can interact each other so that formation of sparingly soluble homo-dimers may occur, especially in the neighbouring pHi value (9.77). A solvent mixture with a lower hydrophilic character, such as 70% water/30% TFE, prevents hydrophobic interactions and increases the ε-subunit solubility.

As for the two truncated sequences present in the *t*-Boc peptide, the hydrophobic residue percentages (Ac-L^{14}-K^{61}: 41%, Ac-S^{9}-K^{61}: 37%) slightly higher than that of the ε-subunit (31%) did not allow separation by RP-HPLC (the conformation of each peptide under acidic conditions could lead to an identical global hydrophobicity). When the *t*-Boc peptide was solubilized in 70% water/30% TFE, the SEC study revealed that the presence of few truncated sequences was sufficient to cause the ε-subunit insolubility (compare Figure 8b with Figure 8a).

Due to its amphiphilic nature SDS can form complexes with hydrosoluble or membrane proteins. Several models have been proposed to explain the SDS/peptide interactions [22]. These interactions are dependent on peptide sequence and certainly are of hydrophobic nature. In our case SDS (200 mM in water), by virtue of its alkyl chain, allows the hydrophobic parts of the truncated sequences and the ε-subunit to hide. Thereby, the dimerization process does not occur.

In summary, to obtain a clear and stable ε-subunit solution at a 3 mM concentration where the pure peptide obtained from the Fmoc-based chemical synthesis is folded, 70% water/30% TFE or 200 mM SDS mixtures at acid pH have to be employed.

Acknowledgements

We thank Dr Jean Velours (IBGC, Université Bordeaux 2, France) for his help concerning the extraction and over-expression techniques and Dr Maya Belghazi (IECB, France) for ESI mass spectrometry measurements.

REFERENCES

1. Senior AE. The proton-translocating ATPase of *Escherichia coli*. *Annu. Rev. Biophys. Biophys. Chem.* 1990; **19**: 7–41.
2. Boyer PD. The ATP synthase — a splendid molecular machine. *Annu. Rev. Biochem.* 1997; **66**: 717–749.
3. Boyer PD, Kohlbrenner WE. In *Energy Coupling in Photosynthesis*. Elsevier: Amsterdam, 1981; 231–240.
4. Cox GB, Cromer BA, Guss JM, Harvey I, Jeffrey PD, Solomon RG, Webb DC. Formation *in vivo*, purification and crystallization of a complex of the γ- and ε-subunits of the F_OF_1-ATPase of *Escherichia coli*. *J. Mol. Biol.* 1993; **229**: 1159–1162.
5. Abrahams JP, Leslie AG, Lutter R, Walker JE. Structure at 2.8 Å resolution of F_1-ATPase from bovine heart mitochondria. *Nature* 1994; **370**: 621–628.
6. Karrasch S, Walker JE. Novel features in the structure of bovine ATP synthase. *J. Mol. Biol.* 1999; **290**: 379–384.
7. Capaldi RA, Schulenberg B, Murray J, Aggeler R. Cross-linking and electron microscopy studies of the structure and functioning of the *Escherichia coli* ATP synthase. *J. Exp. Biol.* 2000; **203**: 29–33.
8. Gibbons C, Montgomery MG, Leslie AG, Walker JE. The structure of the central stalk in bovine F_1-ATPase at 2.4 Å resolution. *Nature Struct. Biol.* 2000; **7**: 1055–1061.
9. Noji H, Yasuda R, Yoshida M, Kinosita K Jr. Direct observation of the rotation of F_1-ATPase. *Nature* 1997; **386**: 299–302.
10. Stock D, Leslie AG, Walker JE. Molecular architecture of the rotary motor in ATP synthase. *Science* 1999; **286**: 1700–1705.
11. Sambongi Y, Iko Y, Tanabe M, Omote H, Iwamoto-Kihara A, Ueda I, Yanagida T, Wada Y, Futai M. Mechanical rotation of the c-subunit oligomer in ATP synthase (F_1F_O): direct observation. *Science* 1999; **286**: 1722–1724.
12. Arselin G, Gandar JC, Guérin B, Velours J. Isolation and complete amino acid sequence of the mitochondrial ATP synthase ε-subunit of the yeast *Saccharomyces cerevisiae*. *J. Biol. Chem.* 1991; **266**: 723–727.
13. Guélin E, Chevallier J, Rigoulet M, Guérin B, Velours J. ATP synthase of yeast mitochondria. Isolation and disruption of the ATP ε-gene. *J. Biol. Chem.* 1993; **268**: 161–167.
14. Nesterenko MV, Tilley M, Upton SJ. A simple modification of Blum's silver stain method allows for 30 minutes detection of proteins in polyacrylamide gels. *J. Biochem. Biophys. Methods* 1994; **28**: 239–242.
15. Johnson WC Jr. Protein secondary structure and circular dichroism: a practical guide. *Proteins: Struct. Funct. Gen.* 1990; **7**: 205–214.
16. Lu H, Buck M, Radford SE, Dobson CM. Acceleration of the folding of hen lysozyme by trifluoroethanol. *J. Mol. Biol.* 1997; **265**: 112–117.
17. Penin F, Deleage G, Gagliardi D, Roux B, Gautheron DC. Interaction between δ- and ε-subunits of F_1-ATPase from pig heart mitochondria. Circular dichroism and intrinsic fluorescence of purified and reconstituted $\delta\varepsilon$ complex. *Biochemistry* 1990; **29**: 9358–9364.
18. Regnier FE, Gooding KM. High-performance liquid chromatography of proteins. *Anal. Biochem.* 1980; **103**: 1–25.
19. Alexandrescu AT, Ng YL, Dobson CM. Characterization of a trifluoroethanol-induced partially folded state of α-lactalbumin. *J. Mol. Biol.* 1994; **235**: 587–599.
20. Schonbrunner N, Wey J, Engels J, Georg H, Kiefhaber T. Native-like β-structure in a trifluoroethanol-induced partially folded state of the all-β-sheet protein tendamistat. *J. Mol. Biol.* 1996; **260**: 432–445.
21. Kyte J, Doolittle RF. A simple method for displaying the hydropathic character of a protein. *J. Mol. Biol.* 1982; **157**: 105–135.
22. Lu L, Lundhal P. Quantitative micellar chromatographic analysis of interaction between peptides and sodium dodecyl sulfate micelles. *J. Chromatogr. A* 1996; **741**: 49–57.

